Supplemental material for

DOXORUBICIN IMPACTS THE CHROMATIN BINDING OF HMGB1, HISTONE H1 AND RETINOIC ACID RECEPTOR

Rosevalentine Bosire[1,2], Lina Fadel[1,3], Gábor Mocsár[1], Péter Nánási[1], Pialy Sen[1,3], Anshu Kumar Sharma[1], Muhammad Umair Naseem[1,3], Attila Kovács[4], Jennifer Kugel[5], Guido Kroemer[6,7,8,9,10], György Vámosi[1*] & Gábor Szabó[1*]

[1]Department of Biophysics and Cell Biology, Faculty of Medicine, University of Debrecen, Debrecen, Hungary
2Doctoral School of Molecular Cell and Immune Biology, University of Debrecen, Debrecen, [3]Doctoral School of Molecular Medicine, University of Debrecen, Debrecen, Hungary
Hungary
[4]Department of Radiation Therapy, Faculty of Medicine, University of Debrecen, Debrecen, Hungary
[5]Department of Biochemistry, University of Colorado, Boulder
[6]Centre de Recherche des Cordeliers, Equipe labellisée par la Ligue contre le cancer, Université de Paris, Sorbonne Université, Paris, France
[7]Metabolomics and Cell Biology Platforms, Institut Gustave Roussy, Villejuif, France
[8]Pôle de Biologie, Hôpital Européen Georges Pompidou, Paris, AP-HP, France
[9]Suzhou Institute for Systems Medicine, Chinese Academy of Medical Sciences, Suzhou, China. [10]Karolinska Institute, Department of Women's and Children's Health, Karolinska University Hospital, Hospital

*Equal senior, corresponding authors: szabog@med.unideb.hu, vamosig@med.unideb.hu

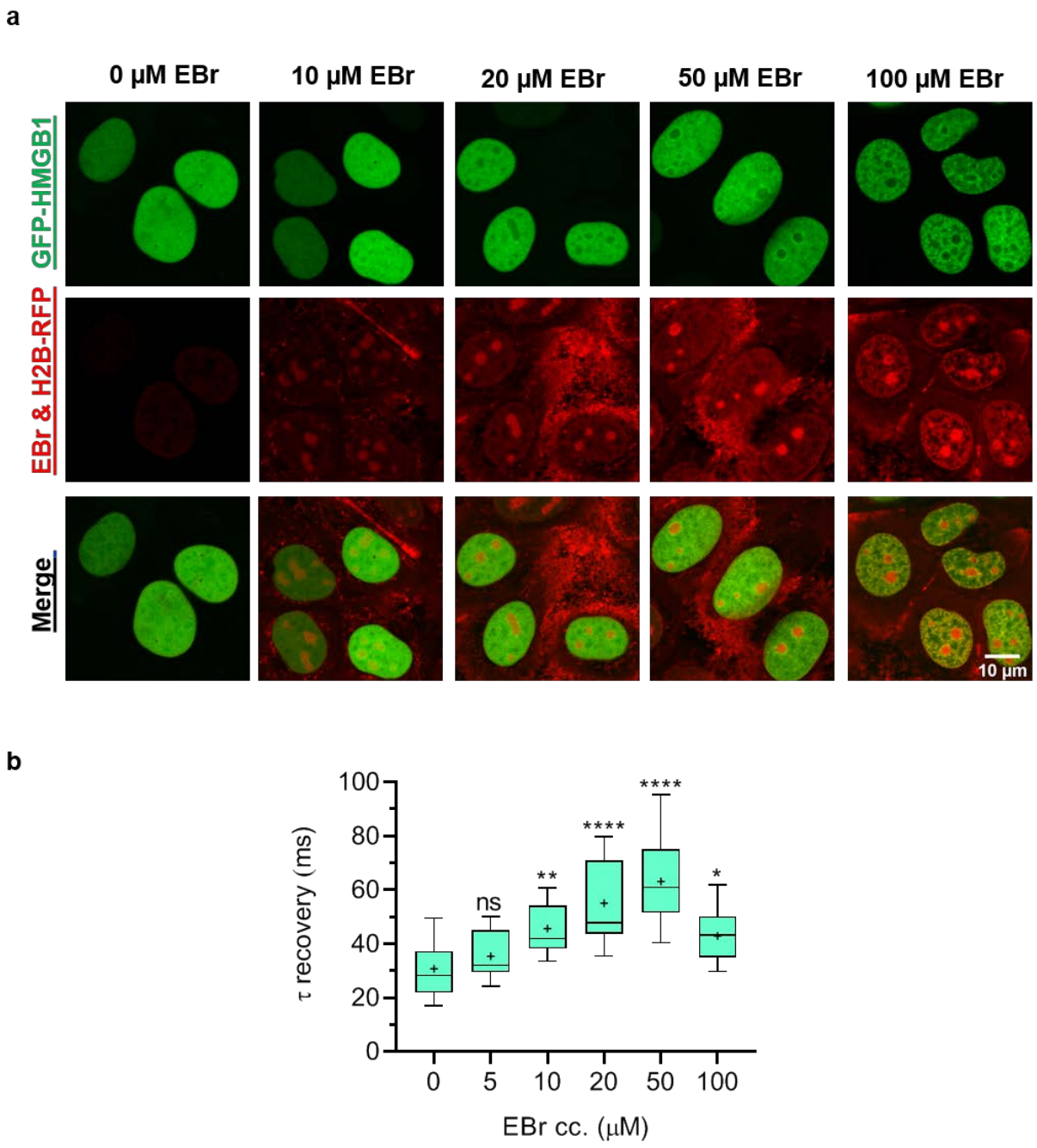

Figure S1: EBr causes redistribution of HMGB1 within the nuclei and exerts a biphasic effect on HMGB1 mobility in live cells. U2OS^{2FP} cells were incubated with 0, 10, 20, 50 and 100 µM EBr for 1 hr and then imaged by confocal microscopy. **a**) Representative nuclei showing GFP-HMGB1, EBr and H2B-RFP and the merged images. Uptake of EBr is evident from the appearance of nucleoli and cytoplasmic fluorescence, as well as increased chromatin fluorescence. At 100 µM EBr, chromatin condensation can also be observed. H2B-RFP hardly contributes to the red signal, therefore the fluorescence gain of that channel in the control sample (0 EBr) was increased on the image to make H2B-RFP visible. Following EBr treatment, there is gradual loss of GFP from the nucleoli and its distribution in chromatin becomes more structured **b**) Fluorescence recovery time of GFP-HMGB1 in EBr treated cells as measured by point FRAP. Following treatment with EBr, GFP-HMGB1 recovery time increases peaking at 50 µM. One-way ANOVA with post hoc Dunnett's test was used to calculate significance of differences relative to 0 EBr. *p< 0.05, **p<0.01, ****p<0.0001.

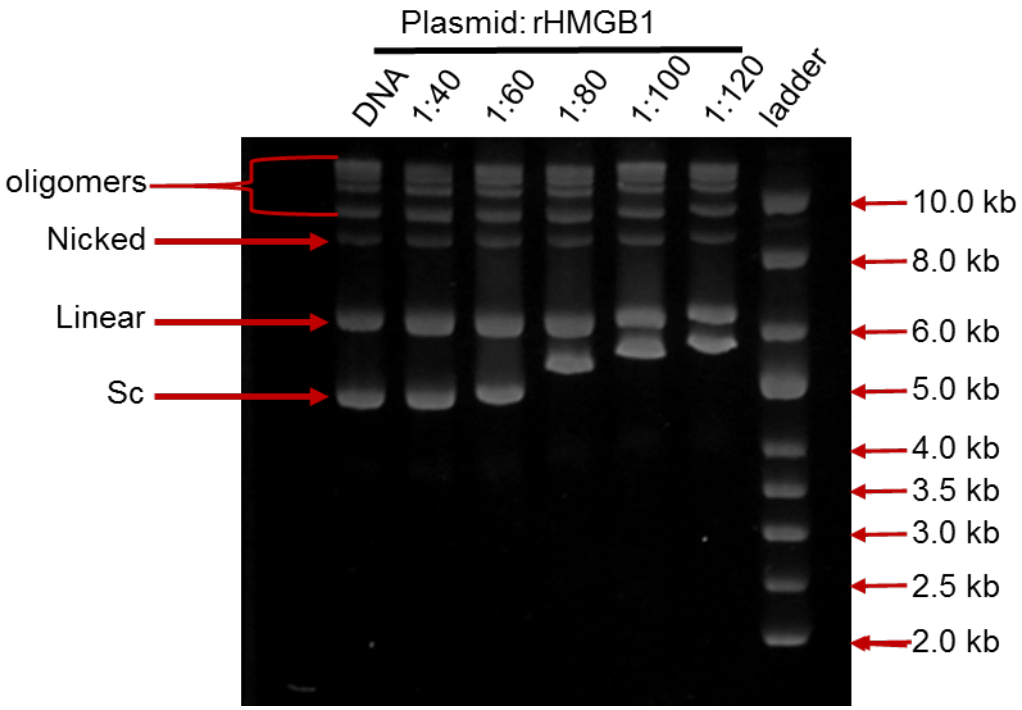

Figure S2: Varying amounts of rHMGB1 were added and allowed to bind 1.5 µg of plasmid DNA containing nicked, linear and supercoiled forms in equal amounts, before being separated by gel elecrophoresis. The gel was stained with 0.5 µg/ml EBr following electrophoresis.

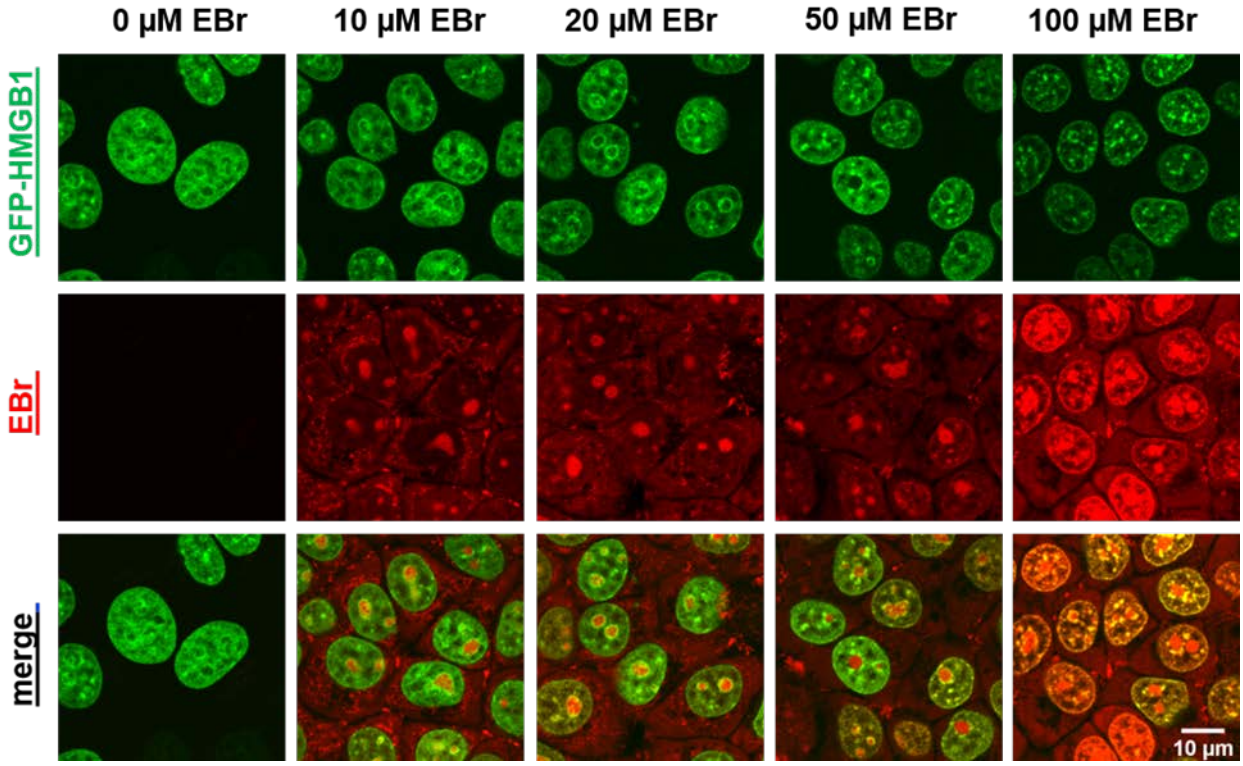

Figure S3: EBr displaces histone H1c from chromatin. Live HeLa cells expressing GFP tagged histone H1c were treated for 1 hr with varying concentrations of EBr. Representative nuclei from EBr treated cells are shown.

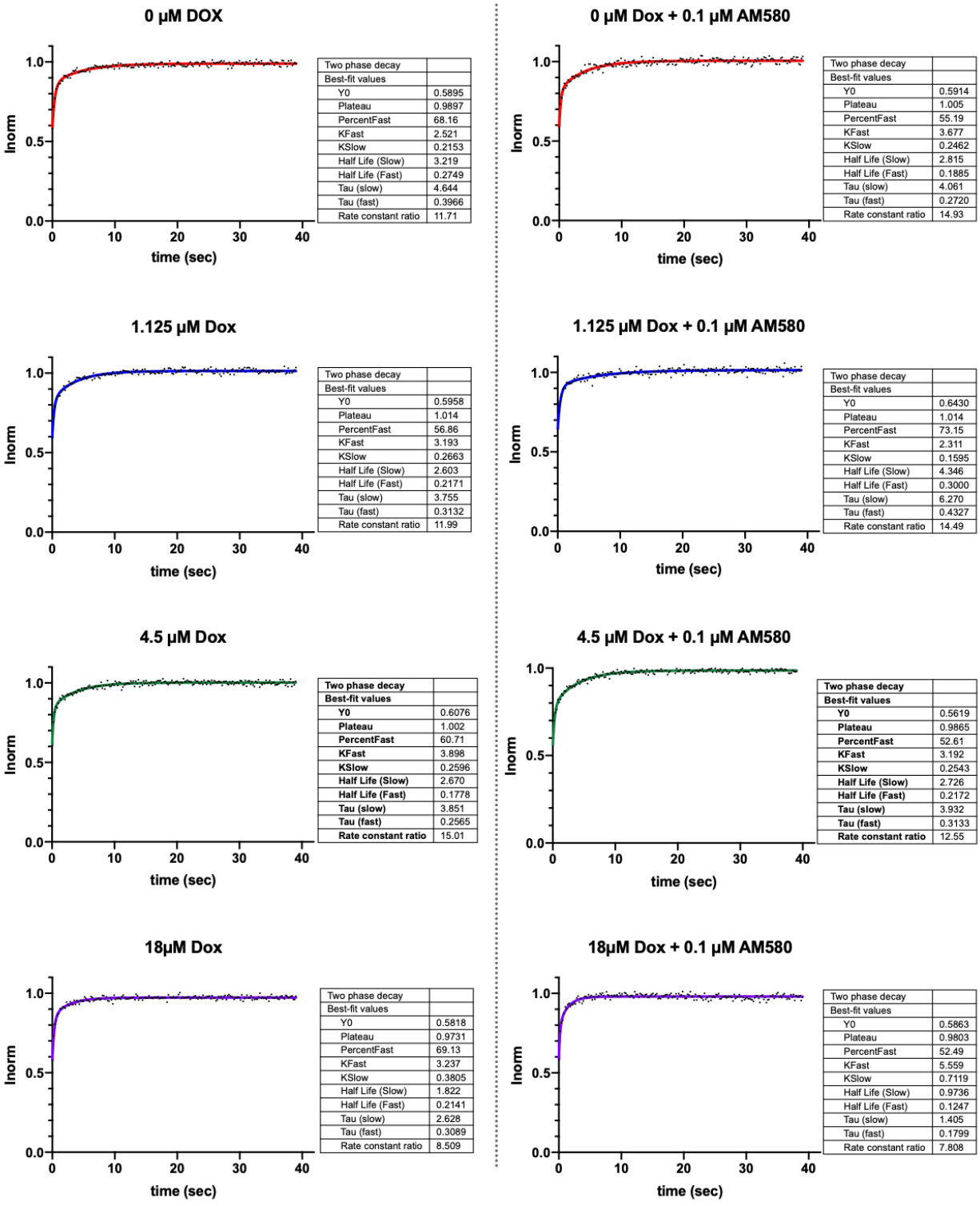

Figure S4: Representative two-component exponential fits of EGFP-RARα normalized intensities using GraphPad Prism version 8.4.0. The curves represent EGFP-RARα normalized intensities at different concentrations of doxorubicin (0, 1.125, 4.5, 18 µM) in the presence or absence of RARα specific agonist treatment, 0.1 µM AM580.

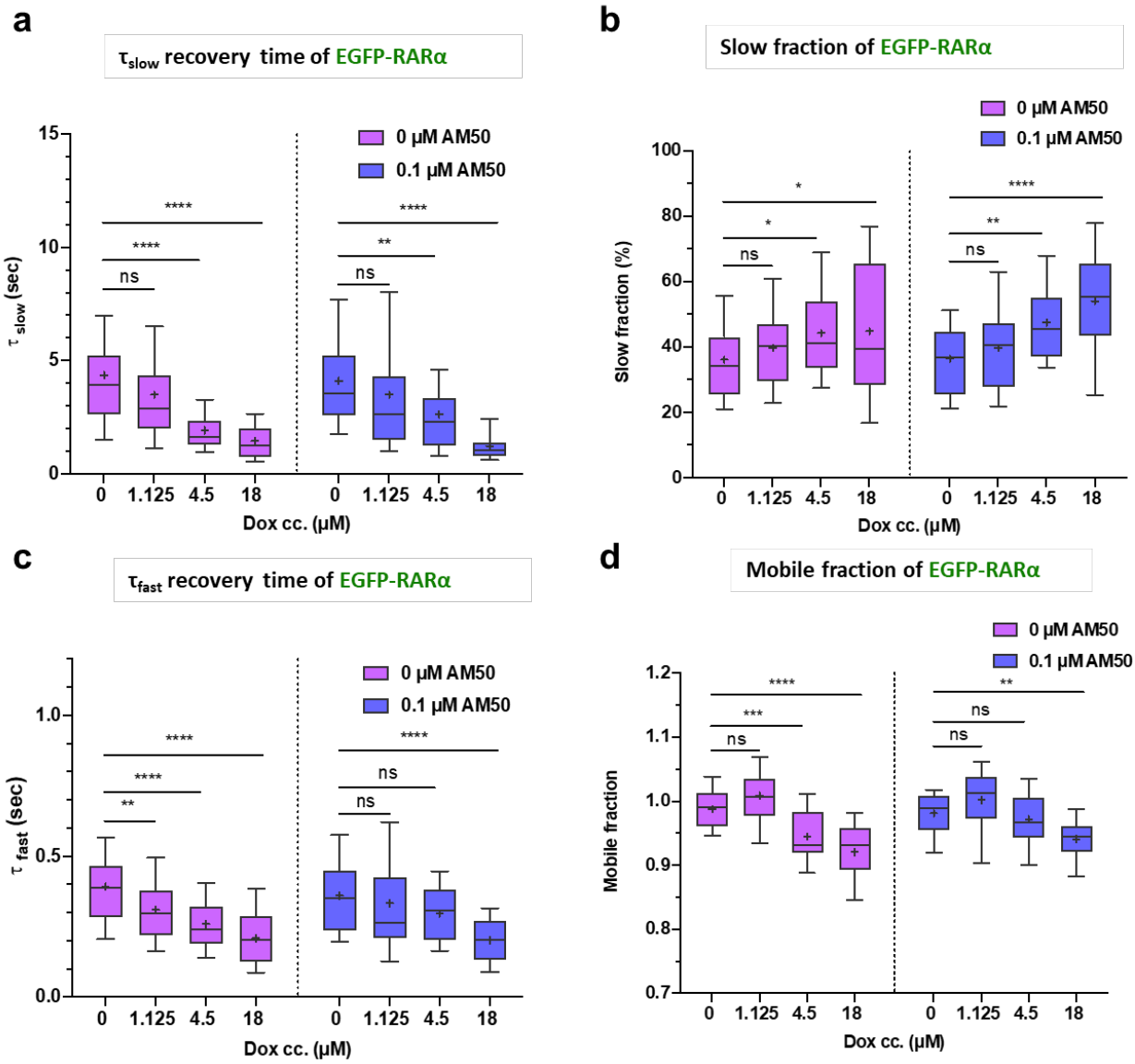

Figure S5: Recovery times and fractions of the slow and fast components of EGFP-RARα expressed in HeLa cells from the strip FRAP experiments. (a) Recovery times of the slow component in cells treated with the indicated concentrations of Dox and/or RAR agonist AM580; (b) fractions of the slow component; (c) recovery times of the fast component; (d) fraction of the mobile component. In the figures, the p values are defined by Tukey's multiple comparison test where, *($p<0.5$), **($p<0.1$), ***($p<0.01$), ****($p<0.001$), ns, not significant.

Dox had no effect on EGFP dimer diffusion

Dox has previously been shown to alter the overall chromatin structure through core histone eviction and histone aggregation [1,2]. Such an altered environment may affect the microviscosity of the nucleus allowing for faster diffusion. To learn if reduced FRAP recovery times of RARα (Fig. 5) reflect reduced binding or decreased viscosity, the effect of Dox on diffusion of EGFP dimers, having no known binding sites on chromatin, was measured. Dox had no effect on its recovery time (Fig. S6) indicating that the average microviscosity in the nucleus did not change to an extent that would influence the diffusion of proteins of this size (EGFP dimer: ~54 kDa, EGFP-RAR: 78 kDa) in the nucleus. Thus, the reduced FRAP recovery time of RARα indeed reflects reduced binding. We also measured the local mobility of EGFP dimers by FCS. The FCS-derived D value displayed no significant change upon 4.5 µM Dox treatment either (Fig. S7c).

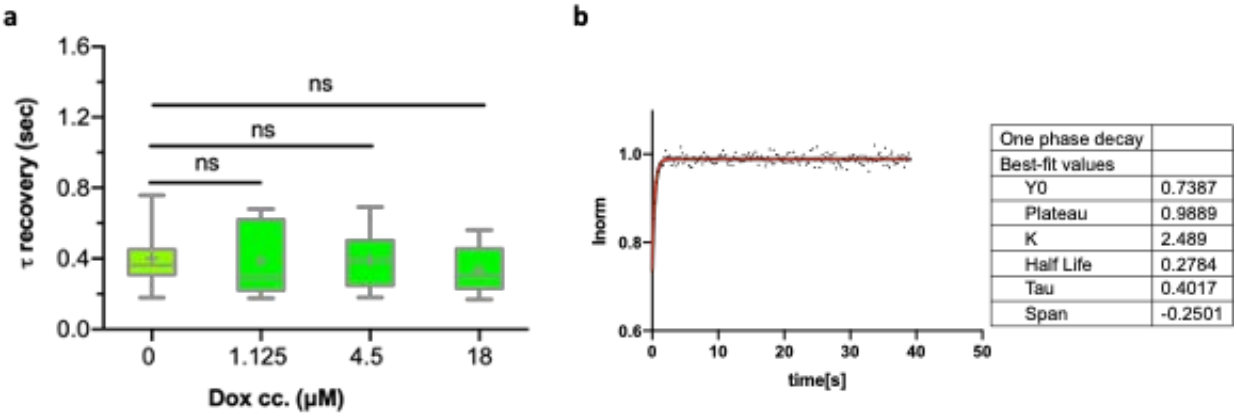

Figure S6: Nuclear mobility of EGFP dimer is unaffected by Dox treatment. Recovery time of an inert protein, EGFP dimer as a control for FRAP experiments. (**a**) $\tau_{average}$ recovery times for the EGFP dimer at different concentrations of doxorubicin (0, 1.125, 4.5, 18 µM). (**b**) Representative one-component exponential decay fit of the normalized intensity of the EGFP dimer. One-way ANOVA with post hoc Dunnett's test was used to calculate significance *p<0.05.

1 Imre, L. *et al.* Nucleosome stability measured in situ by automated quantitative imaging. *Sci Rep* **7**, 12734, doi:10.1038/s41598-017-12608-9 (2017).

2 Nanasi, P., Jr. *et al.* Doxorubicin induces large-scale and differential H2A and H2B redistribution in live cells. *PLoS One* **15**, e0231223, doi:10.1371/journal.pone.0231223 (2020).

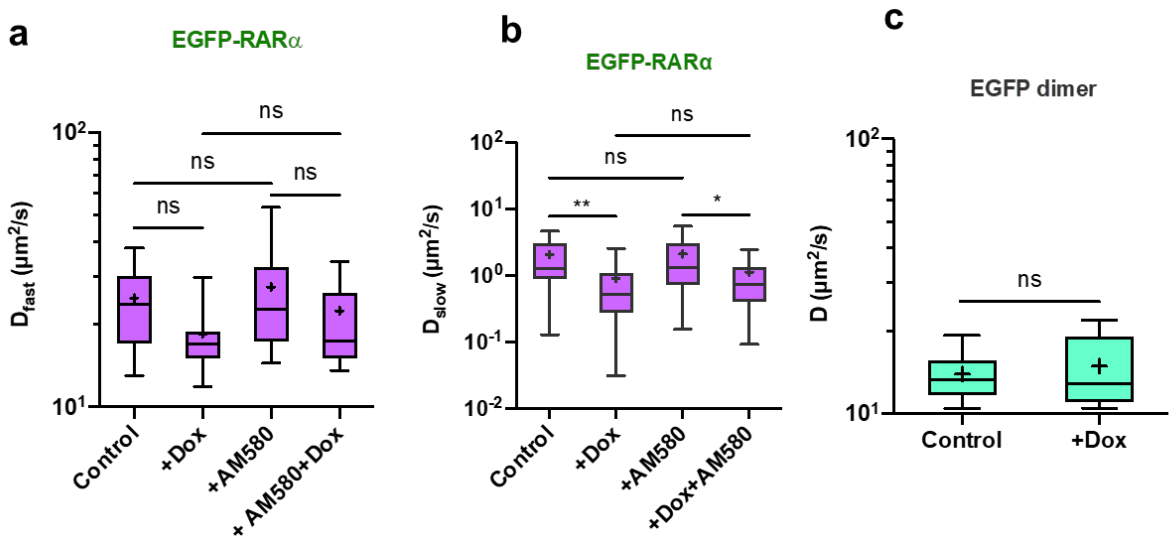

Figure S7: Diffusion constants of EGFP-RARα and EGFP dimer. Diffusion constants of **a)** the fast, freely diffusing or transiently DNA-bound component of EGFP-RARα and **b)** the slow, DNA-bound component in control and Dox-treated (4.5 µM) HeLa cells stably expressing the receptor. The increased variability of D_{slow} in Dox-treated cells may reflect the more heterogeneous distribution of GFP-RARα as shown in Fig. 6. **c)** The diffusion constant of the EGFP dimer did not change significantly. Two-way ANOVA with Tukey's multiple comparison test was used to calculate significance; *p<0.05, **p<0.01, ns, not significant.

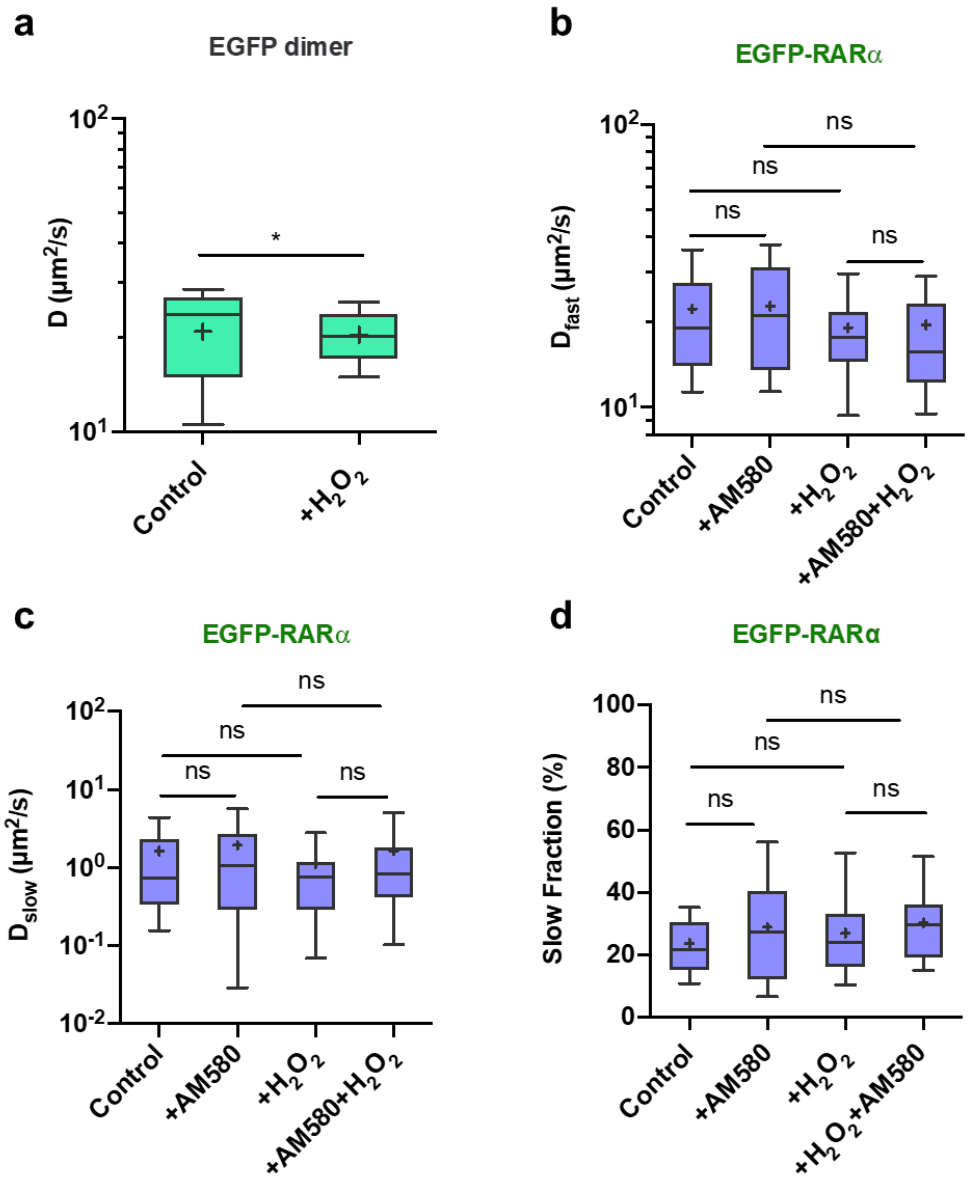

Figure S8: H_2O_2 has no effect on DNA-binding and diffusion of RARα in HeLa cells. Diffusion properties of EGFP-RARα and the inert protein EGFP dimer as a control were measured by FCS. (**a**) Diffusion coefficient of EGFP dimer upon H_2O_2 treatment. (**b**) Diffusion coefficient of freely diffusing EGFP-RARα (fast component) and (**c**) DNA-bound EGFP-RARα (slow component). (**d**) Fraction of DNA-bound EGFP-RARα (slow component). p values are defined by Tukey's multiple comparison test where, *($p<0.5$), **($p<0.1$), ***($p<0.01$), ****($p<0.001$), ns, not significant.

a EGFP dimer

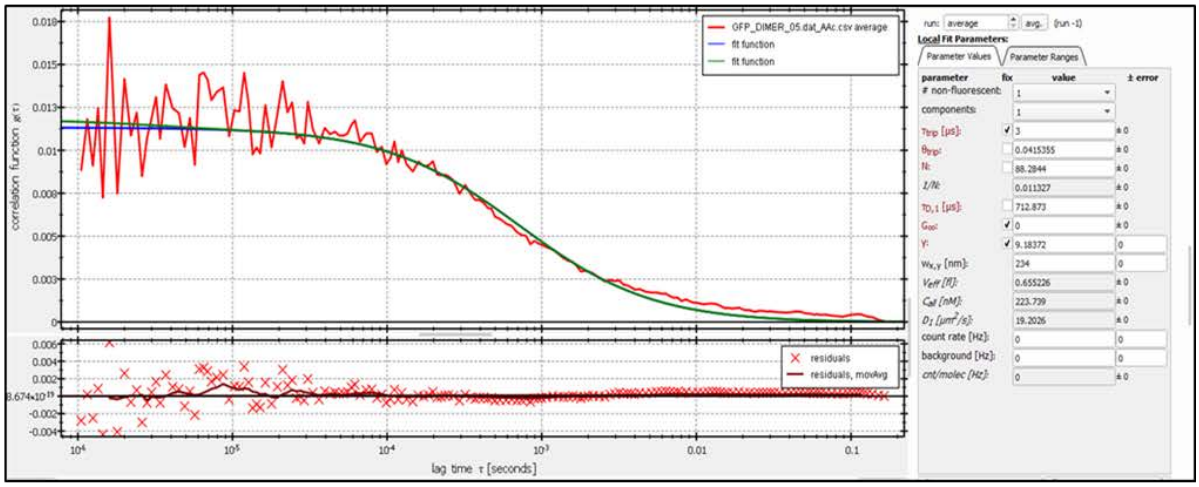

b EGFP dimer + H_2O_2

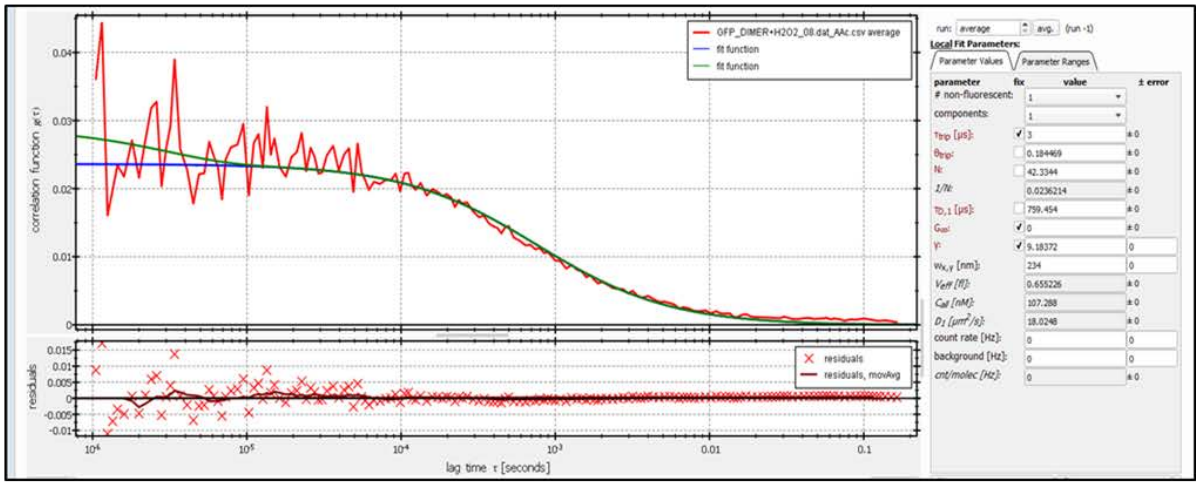

c EGFP-RARα + AM580

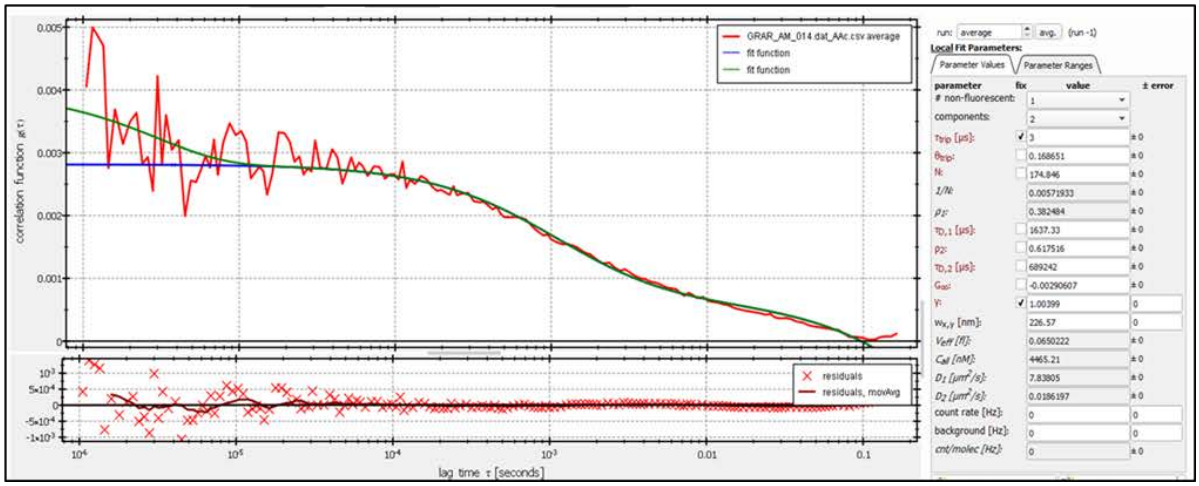

d EGFP-RARα + AM580 + H_2O_2

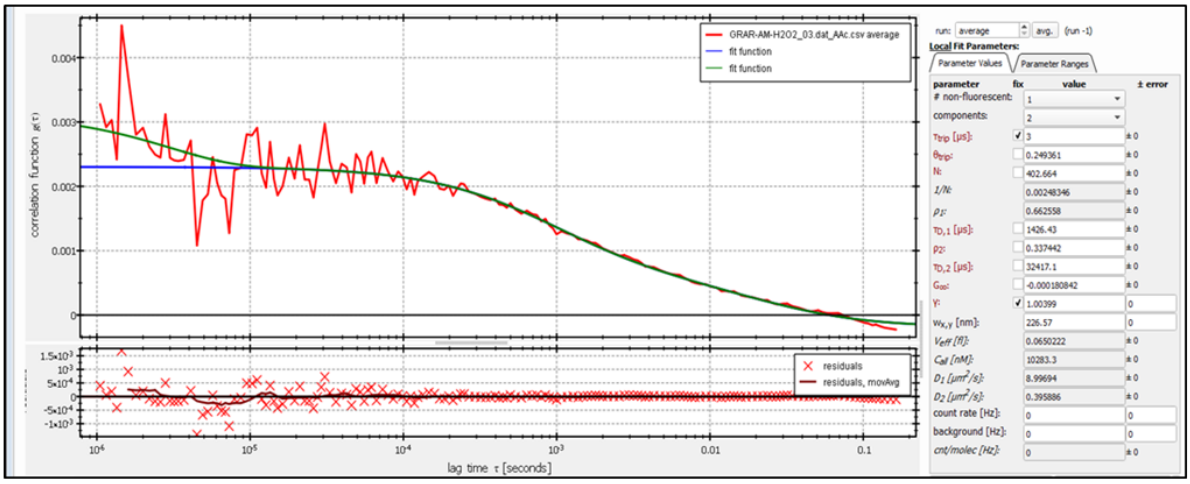

e EGFP-RARα

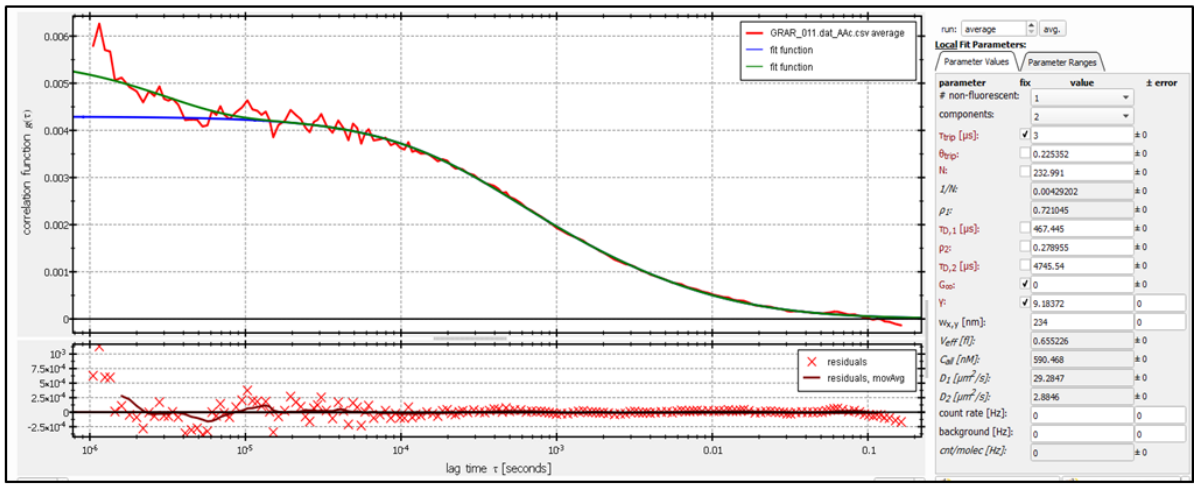

f EGFP-RARα + H_2O_2

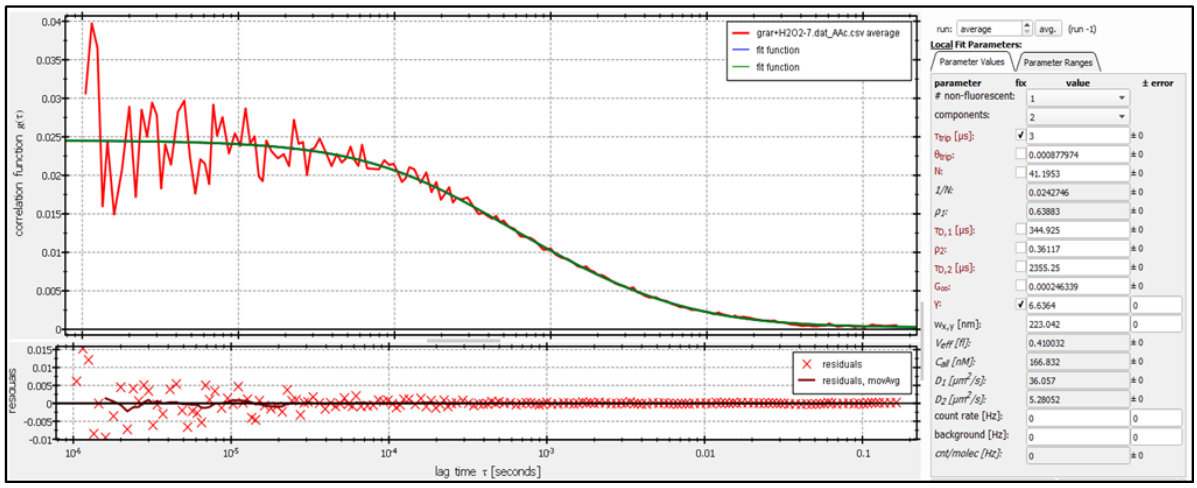

Figure S9: Autocorrelation curves of EGFP dimer and EGFP-RARα in control and H_2O_2 / AM580 treated HeLa cells. (**a-b**) Raw average autocorrelation curves from 10×8 s runs (red) fit to a model with one diffusion component, with (green) or w/o triplet term (blue) of the EGFP dimer used as control. Below, fit residuals, on the right, fit parameters are shown. (**c-f**) Autocorrelation curves of EGFP-RARα. Treatments with H_2O_2 (200 µM, 20 min) and/or AM580 RAR agonist (100 nM, 30 min) are indicated above the panels.

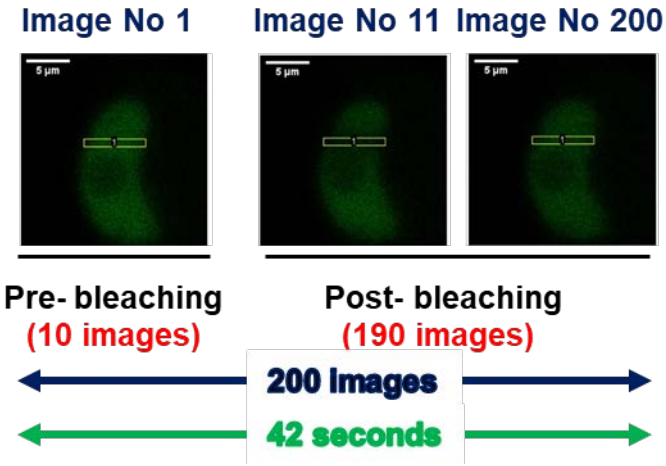

Figure S10: Representative confocal microscopic images showing the applied FRAP settings. Cells expressing EGFP-RARα before bleaching, directly after bleaching and at the end of the time series. In this setting: in 42 s, 200 images were collected as follows: 10 images before bleaching, and 190 images after bleaching.